Chapter 4

Satellite Gravimetry: Mass Transport and Redistribution in the Earth System

Shuanggen Jin

Additional information is available at the end of the chapter

http://dx.doi.org/10.5772/51698

1. Introduction

The Earth's gravity field is a basic physical parameter, which reflects mass transport and redistribution in the Earth System. It not only contributes to study the Earth's interior physical state and the dynamic mechanism in geophysics, but also provides an important way to research the Earth's interior mass distribution and characteristics. The gravity field and its changes with time is of great significance for studying various geodynamics and physical processes, especially for the dynamic mechanism of the lithosphere, mantle convection and lithospheric drift, glacial isostatic adjustment (GIA), sea level change, hydrologic cycle, mass balance of ice sheets and glaciers, rotation of the Earth and mass displacement [33; 37; 7; 39; 17 and 18]. For Geodesy, the gravity field is an important parameter to study the size and shape of the Earth. Meanwhile the Earth's gravity field is very important to determine the trajectory of carrier rocket, long-range weapons, artificial Earth's satellites and spacecrafts. In addition, the gravity field could provide some signals of pre-, co-, and post-earthquake with mass transport following earthquakes [25; 14]. Therefore, precisely determining Earth's gravity field and its time-varying information are very important in geodesy, seismology, oceanography, space science and national defense as well as geohazards.

The global Earth's gravity field is described by spherical harmonics. The non-rotating part of the potential is mathematically described as [15]:

$$V(\theta,\phi)=\frac{GM}{r}[1+\sum_{n=2}^{\infty}\sum_{m=0}^{n}(\frac{R}{r})^n\tilde{P}_{nm}(\sin\theta)(C_{nm}\cos m\phi+S_{nm}\sin m\phi)] \quad (1)$$

where θ and ϕ are geocentric (spherical) latitude and longitude respectively, $\widetilde{P}_{nm}$are the fully normalized associated Legendre polynomials of degree $n$and order$m$, andC_{nm}, $S_{nm}$are

the numerical coefficients of the model. For the Earth's gravity field model, the potential coefficient of the Earth (C_{nm},S_{nm}) should be determined.

Traditional measurements of Earth's gravity field mainly use three techniques. The first one is the terrestrial gravimeter, while the cost is high and the labor work is hard, and furthermore the temporal-spatial resolution is low. The second one is satellite altimetry, which can estimate the gravity field and geoid over the ocean. However, it is still subject to various errors and temporal-spatial resolutions. The third one is to use the laser ranging of artificial Earth's satellites. Because the satellite orbital motion is largely affected by gravitational force and other non-conservation forces, orbit solutions based on precise satellite tracking observations can estimate the gravity field. While, it only provided long-wavelength gravity field information as such satellite orbits are very high. Combination of these three kinds of techniques can give comprehensive gravity field models, however, the accuracy of the model based on satellite orbit tracking data sharply decrease with the increase of the gravity coefficients' degree. Furthermore, due to the sparse surface gravimetric data, uncertain weighting of various measurements and truncation of the spherical harmonic coefficients, these observations are very difficult to obtain a more precise gravity field model.

With the recent development of the low-earth orbit (LEO) satellite gravimetry, it has greatly increased the Earth's gravity field model's precision and temporal-spatial resolution, particularly recent Gravity Recovery and Climate Experiment (GRACE). Satellite gravimetry is a successful innovation and breakthrough in the field of geodesy, following the Global Positioning System (GPS). Unlike the traditional gravity measurements, such as satellite altimetry and high-altitude orbital perturbation analysis, the most advanced SST (Satellite-to-Satellite Tracking) and SGG (Satellite Gravity Gradiometry) techniques are used to estimate the global high-precision gravity field and its variations. Satellite-to-Satellite Tracking technique includes the so-called high-low satellite-to-satellite tracking (hl-SST) [1] and low-low satellite-to-satellite tracking (ll-SST) [43], which can precisely determine the variation rate of the distance between two satellites. The satellite gravity gradiometric (SGG) technique uses a gradiometer carried on the low-orbit satellite to determine directly the second order derivatives of gravity potential (gradiometric tensor), which can recover the Earth's gravity field precisely. Therefore, the satellite gravimetry has greatly improved the gravity field precision and its applications in geodesy, oceanography, hydrology and geophysics.

2. Gravity field from satellite gravimetry

Since 2000, three gravity satellites missions have been launched and dedicated to gravity field recovery, i.e., CHAMP (Challenging Mini-Satellite Payload for Geophysical Research and Application), GRACE (Gravity Recovery and Climate Experiment) and GOCE (Gravity Field and Steady-state Ocean Circulation Explorer).

2.1. High-low satellite to satellite tracking (hl-SST)

CHAMP satellite has been successfully launched on July 15, 2000 using the hl-SST technical mode, and the high orbit satellites were GPS satellites [29]. CHAMP was a German small satellite mission for geoscientific and atmospheric research and applications. The three primary scientific objectives of the CHAMP mission were to obtain highly precise global long-wavelength features of the static Earth's gravity field and its temporal variation with unprecedented accuracy, crustal magnetic field of the Earth and atmospheric and ionospheric products from GPS radio occultation, including temperature, pressure, water vapour and electron content. The GPS receiver on-board CHAMP and ground-based satellite laser ranging were used to determine the CHAMP's orbit. The three-axes STAR accelerometer measured the non-gravitational accelerations of perturbing CHAMP's orbit. Therefore, the long- to mid-scale Earth's gravity field can be recovered from the above data with an unprecedented accuracy.

2.2. High-low/low-low satellite to satellite tracking (hl-SST/ll-SST)

The Gravity Recovery and Climate Experiment (GRACE), a joint mission of NASA and the German Aerospace Center (DLR), has been launched in March 2002 to recover detailed Earth's gravity field [42; 38]. GRACE has twin satellites with distance of about 220 kilometers and used the typical high-low/low-low satellite-to-satellite tracking (hl-SST/ll-SST) techniques. The primary objective is to obtain extremely high-resolution global Earth's gravity field and its changes with time. The k-band ranging system is used to measure the precise distance change rate between twin satellites. With the accelerometer, the GRACE could determine the gravity field and its change with time. These estimates provide a comprehensive understanding of how mass is distributed globally and how that distribution varies over time in the Earth system.

2.3. High-low satellite to satellite tracking/satellite gravity gradient mode

The Gravity Field and Steady-State Ocean Circulation Explorer (GOCE) mission has been launched on March 17, 2009 with taking high-low satellite-to-satellite tracking and satellite gravity gradiometer (hl-SST/SGG), which is the first satellite mission to employ the concept of gradiometry [8]. The mission objectives are to determine gravity-field anomalies with an accuracy of 10^{-5} ms^{-2} (1 mGal) and the geoid with an accuracy of 1-2 cm, and to achieve a spatial resolution better than 100 km. Unlike the previous two modes, GOCE was equipped with three pairs of ultra-sensitive accelerometers and onboard GPS/GLONASS receiver to determine the exact position of the satellite with high-low satellite-to-satellite tracking mode (hl-SST). The non-conservative forces on the gradiometer such as the linear and angular inertia acceleration produced by the atmosphere drag and the solar radiation pressure can be accurately balanced by a non-conservation control system (Drag-free) Therefore, GOCE could recover the global earth gravity field with higher resolution and higher accuracy.

These satellite gravimetric techniques greatly improved the knowledge about the Earth's gravity field, which could provide more abundant information on mass transport and redis-

tribution in the Earth system. These products will make an important contribution to some key scientific issues of global change, such as global sea level changes, ocean circulation, ice sheets and glaciers mass balance and hydrologic cycle This chapter focuses on the mass transport and redistribution in the Earth system with monthly resolution are derived from approximate 10 years of monthly GRACE measurements (2002 August-2011 December).

3. Mass transport and redistribution

3.1. Terrestrial water storage from GRACE

The GRACE mission was launched in March 2002 and began operating nearly continuously since August 2002 [37]. One of the scientific objectives of the GRACE mission is to produce high-quality terrestrial water storage and ocean mass estimates. GRACE delivers monthly averages of the spherical harmonic coefficients, which are sensitive to fluctuations in continental water storage and the polar ice sheets, as well as changes in atmospheric and oceanic mass distribution [40; 17]. At this point, the terrestrial water storage anomalies over the land can be directly estimated by gravity coefficient anomalies for each month (ΔC_{lm},ΔS_{lm}) (40):

$$\Delta\eta_{land}(\theta,\phi,t)=\frac{a\rho_{ave}}{3\rho_w}\sum_{l=0}^{\infty}\sum_{m=0}^{l}\widetilde{P}_{lm}(\sin\theta)\frac{2l+1}{1+k_l}(\Delta C_{lm}\cos(m\phi)+\Delta S_{lm}\sin(m\phi)) \tag{2}$$

where$\rho_{ave}$is the average density of the Earth, $\rho_w$is the density of fresh water, $a$is the equatorial radius of the Earth, $\widetilde{P}_{lm}$is the fully-normalized Associated Legendre Polynomials of degree $l$and order$m$, $k_l$is Love number of degree l[13],θ is the geographic latitude and$\phi$is the longitude. The precise terrestrial water storages (TWS) are estimated using monthly GRACE solutions (Release-04) from the Center for Space Research (CSR) at the University of Texas, Austin from August 2002 until December 2011, except for June 2003, January 2011 and June 2011 without data. The degree 2 and order 0 (C_{20}) coefficients are replaced from Satellite Laser Ranging (SLR) due to large uncertainties in GRACE coefficients [5]. The degree 1 spherical harmonics coefficients (C_{11}, S_{11}, and C_{10}) are used from 34) and the postglacial rebound (PGR) influences is removed with 23). In addition, since GRACE solutions have larger noise and strips [40; 36], the 500km width of Gaussian filter and de-striping filter are used to mitigate these effects [36]. Thus, about 10 years of global terrestrial water storages (TWS) are estimated from GRACE.

3.2 Ocean bottom pressure from GRACE

Monthly GRACE gravity changes over oceanic regions can be transformed to ocean mass or ocean bottom pressure (OBP) at latitudeθ, longitudeϕ as described by 40):

http://dx.doi.org/10.5772/51698

$$\Delta\eta_{ocean}(\theta,\phi,t)=\frac{a\rho_{ave}}{3\rho_w}\sum_{l=0}^{\infty}\sum_{m=0}^{l}\frac{(2l+1)}{(1+k_l)}W_l\tilde{P}_{lm}(\sin\theta)\begin{Bmatrix}(\Delta C_{lm}(t)+\Delta C_{lm}^{GAD}(t))\cos(m\phi)+\\(\Delta S_{lm}(t)+\Delta S_{lm}^{GAD}(t))\sin(m\phi)\end{Bmatrix} \quad (3)$$

where the variables have the same meaning with equation (2), and W_l is the Gaussian averaging function with increasing$l$. As the coefficients from the GRACE are deviations from a background model, we have to add back the monthly OBP modeled in the GRACE processing. A new OBP product (GAD) is now available by [9]. 4] demonstrated that GRACE could measure the variation in the global mean ocean mass (and hence OBP) quite accurately. 2] found that the seasonal mode of OBP variation in the North Pacific extracted from GRACE data agreed qualitatively with that of an ocean model. Therefore, the reliable monthly OBP time series could be precisely estimated from the most recent GRACE gravity field solutions (Release-04) from the Center for Space Research (CSR) at the University of Texas, Austin [4]. Here monthly grid OBPs are used with a 500-km Gaussian smooth from August 2002 until December 2011, except for June 2003, January 2011 and June 2011 when no solutions exist.

4. Results and Discussions

4.1. Global hydrological cycle

4.1.1. Seasonal changes of Terrestrial water storage

The TWS time series have significant seasonal variations. Amplitude and phase of annual and semi-annual variations at grid points are estimated from GRACE TWS time series (August 2002-December 2011) through the method of least squares fit to a bias, trend, and seasonal period sinusoids as:

$$TWS(t)=A_a\sin(\omega_a t-\varphi_a)+A_{sa}\sin(\omega_{sa}t-\varphi_{sa})+B+C(t-t_0)+\varepsilon(t) \quad (4)$$

where $B$is the constant, $t_0$is on January 1st 2002, $\varphi$is the phase and$A$is the amplitude of period p as 1 and 0.5 years. The GRACE results are further compared with the Global Land Data Assimilation System (GLDAS) model. GLDAS model is a hydrological model, which is jointly developed by the National Aeronautics and Space Administration (NASA) Goddard Space Flight Center (GSFC) and the National Oceanic and Atmospheric Administration (NOAA) National Centers for Environmental Prediction (NCEP) [31]. Figure 1 shows the annual amplitude and phase of global terrestrial water storages from GRACE and GLDAS model. It has clearly shown that annual amplitude of GRACE-derived terrestrial water storage is up to 20 cm in South America's Amazon River Basin and about 10 cm in the Niger, Lake Chad and Zambezi River Basins in the African continent, the Ganges and the Yangtze River region in Southeast Asia, and in other areas the annual variations of terrestrial water storage are not significant. The annual amplitudes from GRACE have similar patterns with

the GLDAS, but a little larger than GLDAS results as the GLDAS model does not include groundwater. In addition, for the most parts of the world, the terrestrial water storage reaches the maximum in September-October each year, and the minimum in March-April. The semi-annual signals in most regions of the world are not significant, so here we don't discuss.

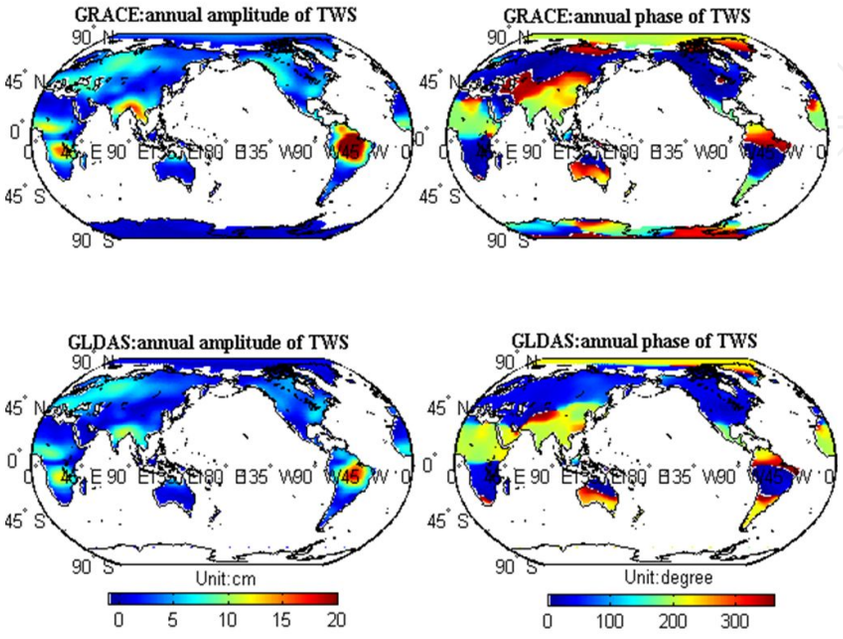

Figure 1. Annual amplitude and phase of TWS based on GRACE and GLDAS model.

4.1.2. Long-term trend of terrestrial water storage

The long-term trends of global terrestrial water storage are further analyzed. Figure 2 shows the long-term trend of global terrestrial water storage from GLDAS and GRACE data. For some parts, they agreed each other, but the GLDAS model cannot capture the detailed extreme climate and human groundwater depletion signals in terrestrial water storage, e.g., great groundwater depletion in Northwest India. While GRACE results in Figure 2(b) have clearly shown that the terrestrial water storage is decreasing at about -15.5 mm/y in Northwest India, which have been proved that over groundwater depletion lead to decrease in TWS [32]. The terrestrial water storage in North China Plain is reducing at -4.8mm/yr, mainly due to the sparse vegetation of the region, the larger evaporation and huge groundwater depletion. While in Antarctica, Greenland and Canadian Archipelago, Alaska, Patagonia glaciers as well as the Himalayan glaciers, the TWS is significantly decreasing due to rapid glacier melting. In addition, the flood in Amazon River Basin of South America, results in increase of terrestrial water storage at about 20.5mm/yr. In La Plata region, the terrestrial water storage is reducing at about -9.8mm/y due to recent drought. Our results almost confirmed the early results based on short-time GRACE data. For example, 39) found that the mass of the Antarctic ice sheet in decreased significantly during 2002–2005, at a rate of 152 ± 80 cubic kilometers of ice per year, which is equivalent to 0.4 ± 0.2 millimeters of global sea-

level rise per year, Luthcke's studies show that during 2002-2005, the Greenland ice sheet lost at the speed of (239 ± 23) km^3 /year [21].

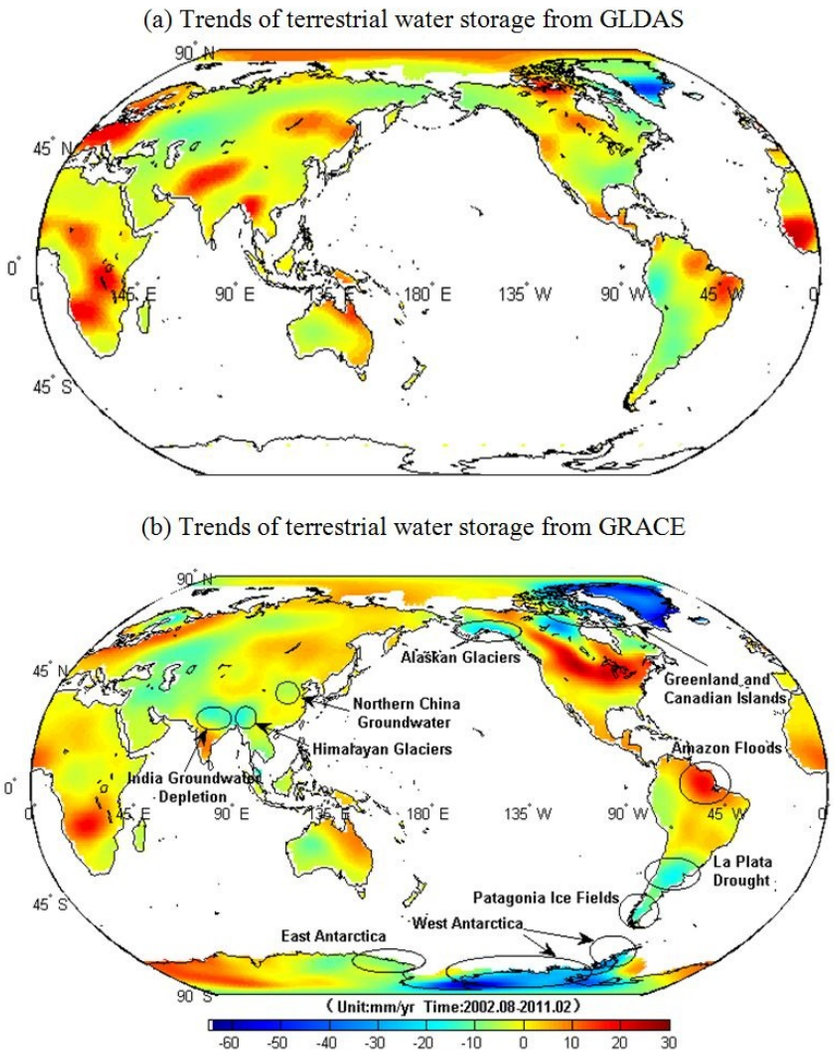

Figure 2. The long-term trend of terrestrial water storage from GLDAS and GRACE.

4.2 Global Ocean Bottom Pressure variations

4.2.1 Seasonal OBP variation

The OBP time series also have significant seasonal variations. Figure 3 shows the amplitude distributions of annual OBP variations from GRACE and ECCO. Larger amplitudes of annual OBP variations from GRACE are found in the Pacific and Indian oceans with up to 3.5±0.4 cm, particularly in the west of Australia, Pacific sector of the Southern Ocean, and the northwest corner of the North Pacific as well, while the lower annual amplitudes are in Atlantic at

less than 1.0±0.3 cm. However, ECCO estimates for all oceans are generally less than 1.5±0.3 cm, much weaker than GRACE. The phase patterns of annual OBP variations are both closer from GRACE and ECCO. For example, the phase of annual OBP variations both shows an asymmetry in middle north Pacific and south Pacific (Figure 4). The semi-annual OBP variations from GRACE and ECCO are relatively weaker and most semi-annual amplitudes are less than 1.0±0.3 cm.

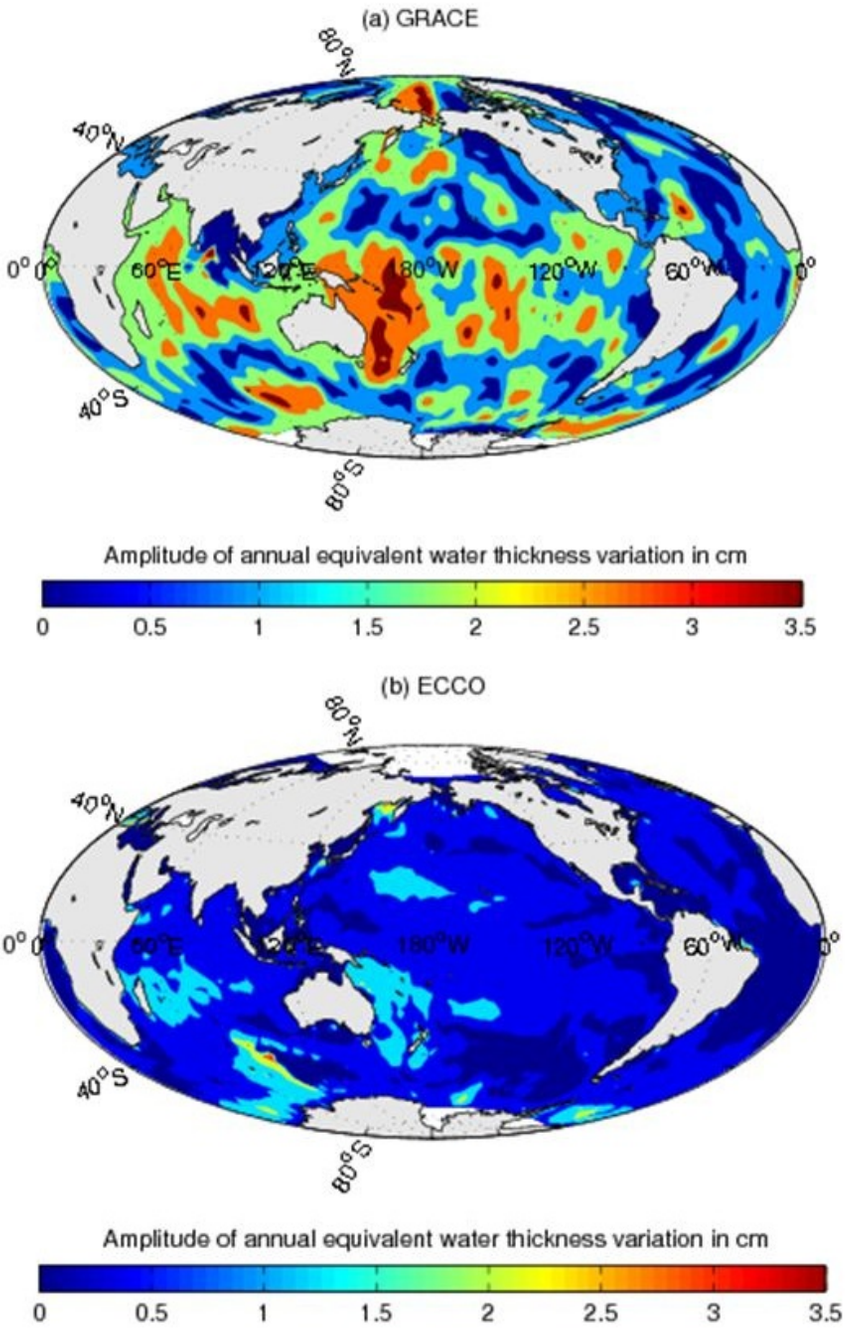

Figure 3. Amplitude of annual OBP variations from GRACE and ECCO.

http://dx.doi.org/10.5772/51698

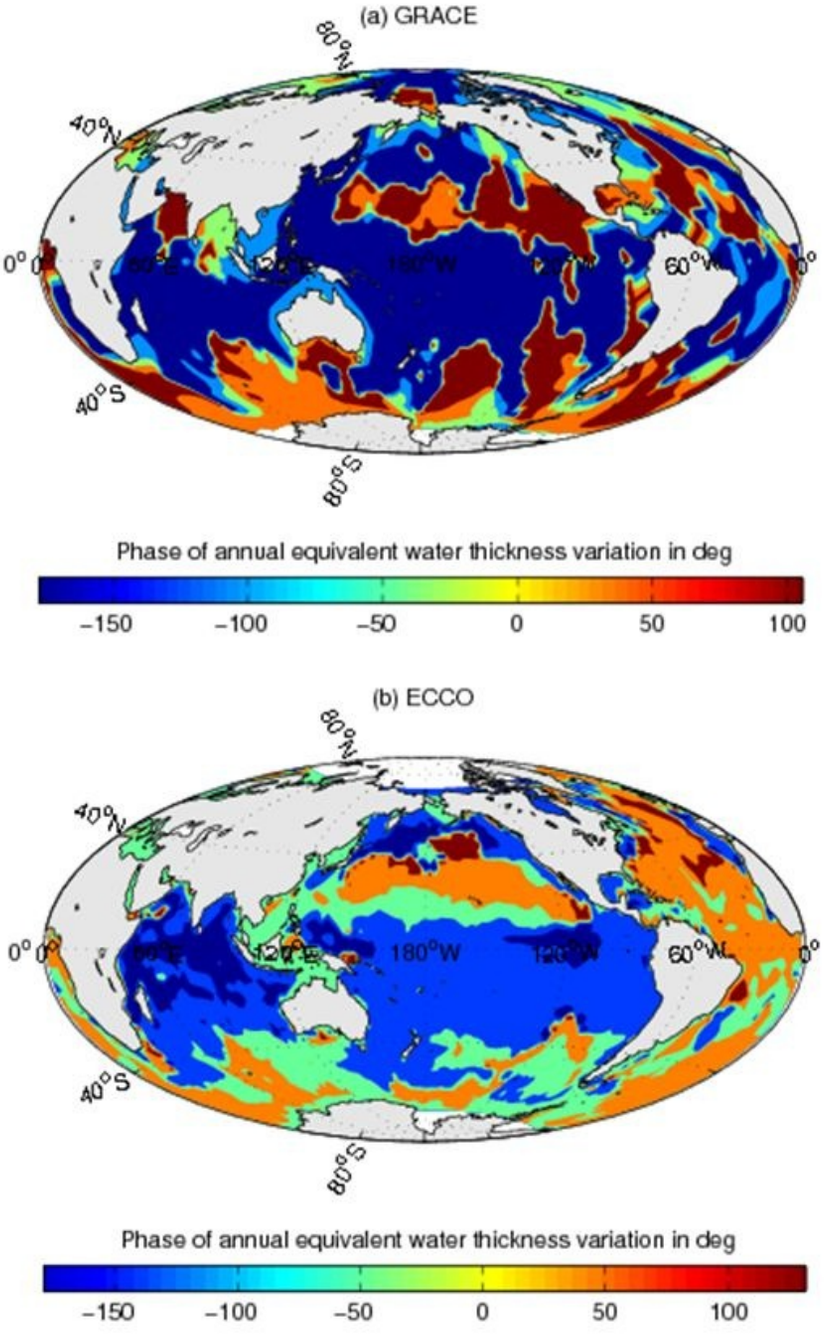

Figure 4. Phase of annual OBP variations from GRACE and ECCO.

4.2.2 Secular OBP variation

Current sea level rise is due mianly to human-induced global warming, which will increase sea level over the coming century and longer periods. One is the steric sea change (i.e. thermal expansion) by the thermal expansion of water due to increasing temperatures, which is well-quantified. The other is non-steric sea level change (i.e. eustatic sea level change) relat-

ed to mass changes through the addition of water to the oceans from the melting of continental ice sheets and fresh water in rivers and lakes. However, the eustatic sea level change is more difficult to predict and quantify due to high uncertain estimates of the Antarctic and Greenland mass and terrestrial water reservoirs. The Satellite-based GRACE observations provide a unique opportunity to directly measure the global ocean mass change (equivalently ocean bottom pressure), which can qualify the OBP change.

The secular OBP variations are analyzed from the almost 10-year monthly GRACE OBP time series (August 2002- December 2011) at 1 ×1 grid. After we check the OBP time series, some anomaly of OBP time series are found between the end of 2004 and early of 2005 near Southeast Asia. Figure 5 shows the non-seasonal mass change time series as the equivalent water thickness in centimeter (cm) at grid point (90.5°E, 2.5°S). It has clearly shown a sudden jump of non-seasonal mass change between the end of 2004 and early of 2005. While two largest earthquakes occurred during these time recorded in about 40 years. One is the Sumatra-Andaman earthquake (Mw = 9.0) on December 26, 2004, and the other one is the Nias earthquake (Mw =8.7) on March 28, 2005. The Sumatra-Andaman earthquake raised islands by up to 20 meters [16] and the ruptures extended over approximately 1800 km in the Andaman and Sunda subduction zones [6]. A number of researchers found gravity anomalies from GRACE before and after the Sumatra-Andaman and Nias earthquakes associated with the subduction and uplift, which agreed with model predictions [e.g., 14]. Therefore, the co-seismic gravity effects should be removed for further analyzing the secular OBP variations.

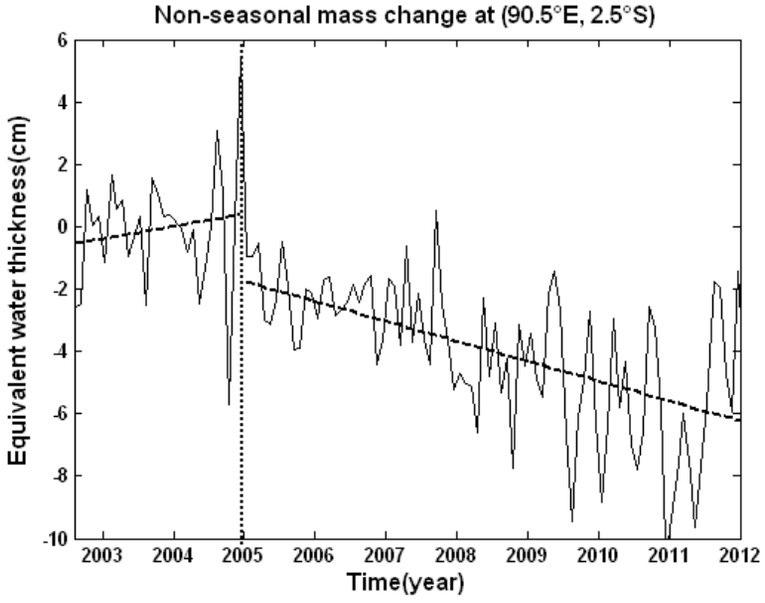

Figure 5. Non-seasonal mass change time series at point (90.5°E, 2.5°S).

Figure 6 shows the trend distribution of secular OBP variations (equivalent water thickness) in cm/yr, ranging from -1.0 to 0.9±0.2 cm/yr, where the upper panel a) is from GRACE and the bottom panel (b) is from ocean model ECCO. Both show significant subsidence of OBP in Atlantic and uplift in northwest Pacific, but the amplitude from GRACE is significantly

http://dx.doi.org/10.5772/51698

larger. The mean OBP time series in Pacific and Atlantic from GRACE and model ECCO also show similar opposite secular OBP variations (Figure 7), reflecting secular exchange of Pacific and Atlantic water. However, the secular change of OBP from GRACE in the Indian sea is subsiding at larger amplitude, while that from ECCO is a little uplift. It needs to be further investigated using long-term satellite observations and other data in the future.

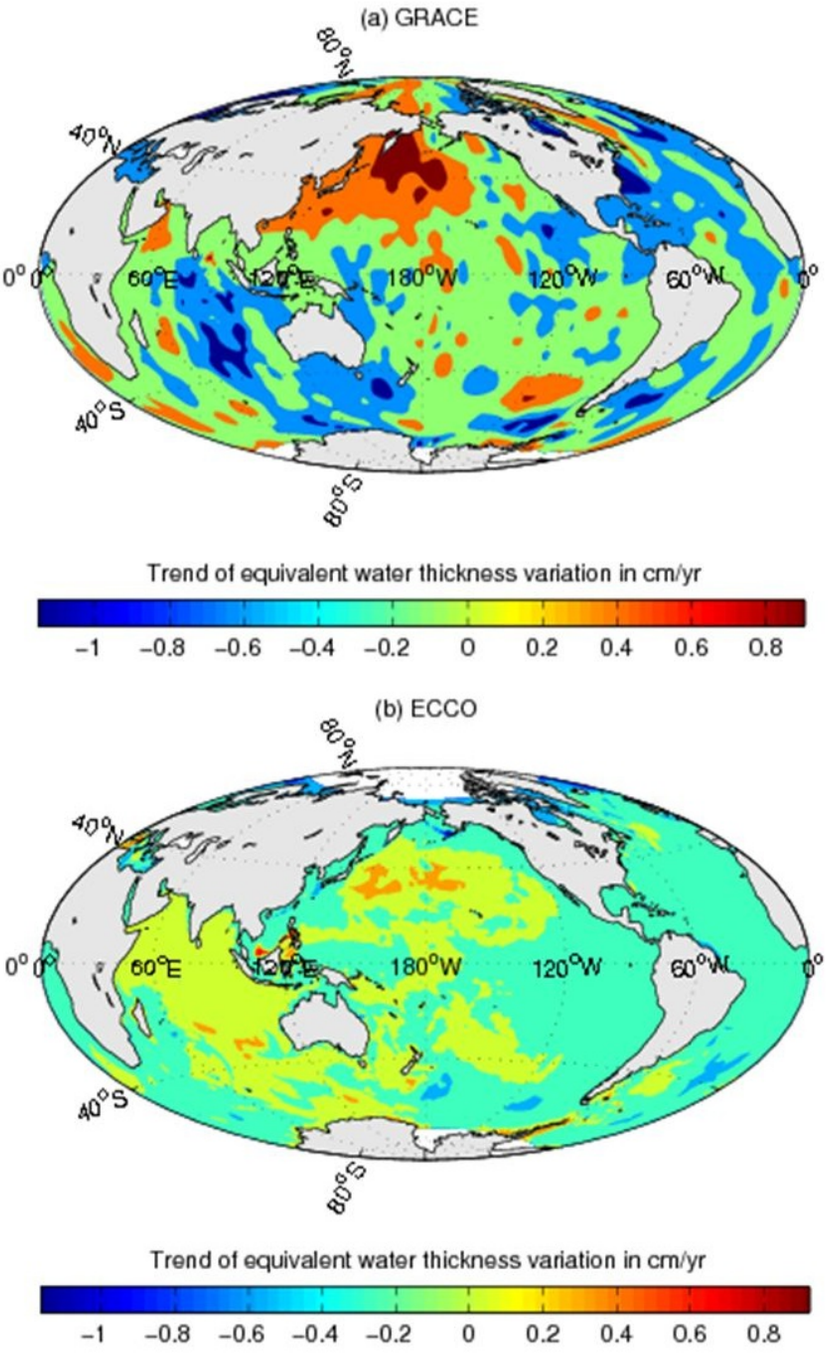

Figure 6. OBP Trend as equivalent water thickness variation in cm/yr.

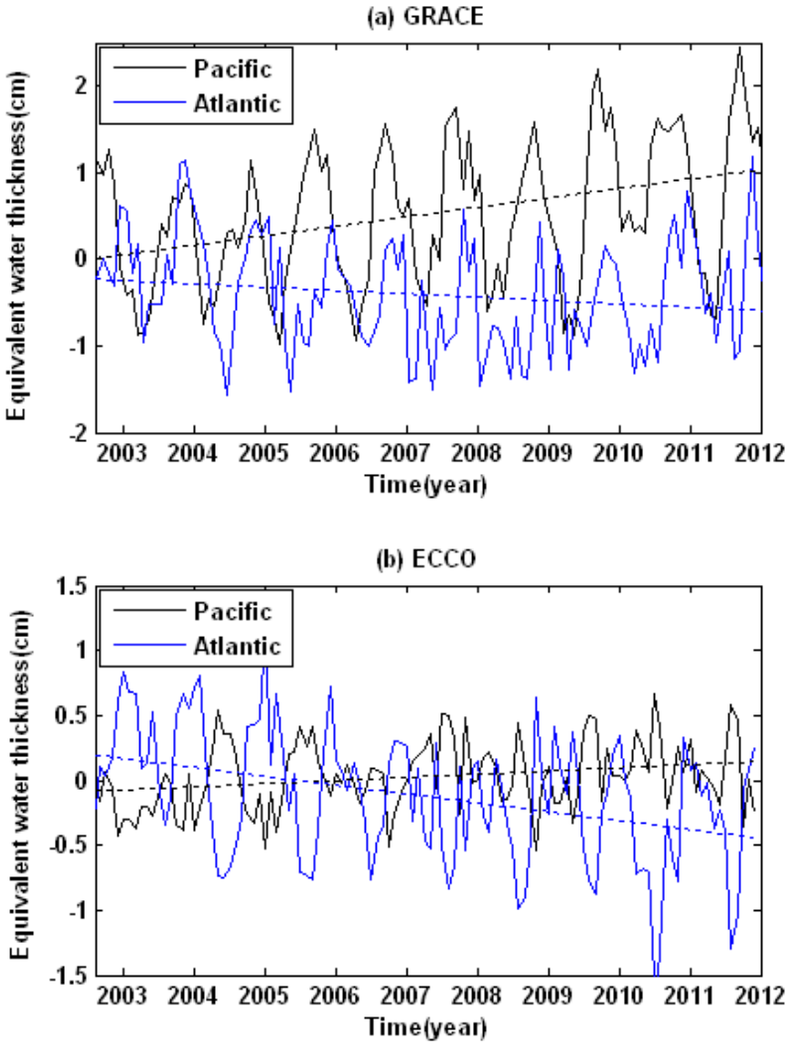

Figure 7. Mean OBP time series from GRACE and ECCO in Pacific and Atlantic.

4.2.3 High frequent OBP variations

The unmodelled OBP residuals (observed minus modelled seasonal terms) reflect the high frequency variation, mainly the high frequent and noise components. We estimate the higher frequency variability by taking the root-mean-square (RMS) of the OBP time series after removing the constant, trend, annual and semi-annual variations as the best-fit sinusoid:

$$RMS = \sqrt{\frac{1}{N}\sum_{t=1}^{N}(OBP_o^t - OBP_M^t)^2} \tag{5}$$

http://dx.doi.org/10.5772/51698

where OBP_o^t is the OBP from GRACE or ECCO at time$t$, $OBP_M^t$is the best fitted value at time t from A*sin(2π(t-t_0)/p +φ)+B+C(t-t_0), and N is the total observation number. The RMS of high-frequency OBP variations at globally distributed grid sites are shown in Figure 8. The high frequency variability of OBP from GRACE ranges from 0 to 3.4 cm with mean amplitude of about 2.0 cm, primarily due to in high frequent OBP variations and noise components of GRACE data processing, while the high frequency variability of OBP from ECCO is ranging from 0 to 2.3 cm with mean amplitude of about 0.7 cm, particularly smaller and smoother in tropical regions. Both have shown the similar higher frequency variability in high-latitude, especially in southern high latitude areas.

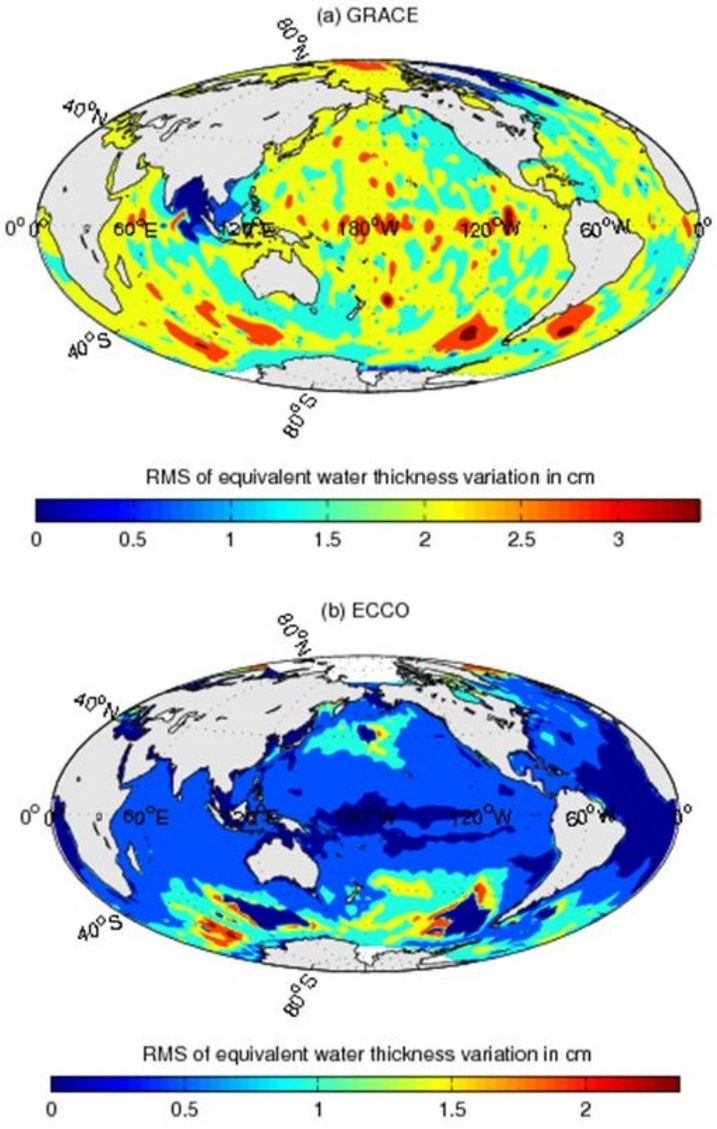

Figure 8. The root-mean-square (RMS) of OBP after removing the constant, trend, annual and semi-annual variations terms.

4.3 Discussions

Although GRACE can well estimate global larger-scale mass transport and redistribution in the Earth system, but it is still subject a number of effects, such as orbital inclination of GRACE, hardware noise and data processing methods. Therefore, the terrestrial water storage and ocean bottom pressure need to be further improved. In addition, the accuracy of geophysical models, post-glacial rebound and tide model also affect the GRACE results. For ocean bottom pressure variation, although 2) found that the seasonal mode of OBP variation in the North Pacific from GRACE data agreed qualitatively with the ocean model, while the secular trend and mean high frequency variability of global OBP from GRACE are higher than that from ECCO by 2-3 times. On one hand, the leakage of land hydrology signals will involve in GRACE-derived OBP estimates (30). Other reasons are the aliasing errors of OBP fluctuations, including atmospheric model and glacial isostatic adjustment (GIA) model. These can affect the tendency, seasonal and high-frequent variations with larger amplitude in the GRACE data than the ECCO estimates, while leakage effect at semi-annual period is less (26), but the GIA will largely affect the OBP trend. In addition, the tides can dealiase errors of 1 cm over most of the oceans [28], and such errors may affect GRACE OBP estimates during non-tidal models corrections. Finally, the instrument noises may affect GRACE solutions [28]. Therefore, one needs to further consider the instrument noise effects and tide aliasing errors in the future.

5. Conclusion

In this Chapter, the mass transport and redistribution in the Earth system are studied using monthly GRACE data. Seasonal and secular changes of global terrestrial water storage in the past 10 years are investigated from GRACE data as well as compared with GLDAS model. The results have shown that the global terrestrial water storages have obvious seasonal changes and long-term trend. The annual amplitude can reach up to 20cm in South America's Amazon River Basin and almost about 10cm in the Niger, Lake Chad and Zambezi River Basins in Africa, the Ganges and the Yangtze River region in Southeast Asia. The maximum terrestrial water storage normally appears in Sep-Oct, and the minimum terrestrial water storage normally appears around in Mar-Apr. The long-term variations of terrestrial water storage are also clear in some areas. For example, the terrestrial water storage is decreasing at about -15.5mm/y in Northwest India due to groundwater depletion, increasing at about 20.5mm/yr in Amazon River Basin of South America due to the flood, and reducing at about -9.8mm/yr in La Plata region due to recent drought. In addition, the secular TWS changes are also significant due to glacier melting, such as in Antarctica, Greenland, Canadian Islands, Alaska, Himalayan and Patagonia glaciers. These results indicate that the satellite gravity could well monitor terrestrial water storage changes and their responses to extreme climate events.

For ocean areas, strong seasonal variability in GRACE OBP at both annual and semi-annual periods are found, coinciding well with model ECCO results but the model amplitudes are

much weaker. Phase patterns tend to match well at annual and semi-annul period. The secular global OBP variations are ranging from -1.0 to 0.9±0.2 cm/yr. The mean OBP time series in Pacific and Atlantic from GRACE and model ECCO both show similar opposite secular OBP variations, reflecting secular exchange of Pacific and Atlantic water. However, the secular change of OBP from GRACE in the Indian sea is down at larger amplitude, while that from ECCO is a little uplift. It needs to be further investigated using long-term satellite observations and other data in the future. In addition, on a global scale, the monthly OBP time series from GRACE have a stronger high-frequent variability than the ocean general circulation model (ECCO), particularly in tropical regions, but both have shown the similar higher frequency variability in high-latitude, especially in southern high latitude areas.

Some uncertainties at the secular, annual, semi-annual and high frequency periods might be from GRACE instruments noises and data processing strategies. It needs to further improve OBP estimates from GRACE by removing data noise from aliasing or combining other data in the future. With the launch of the next generation of gravity satellite with improving the measurement accuracy, data processing methods and geophysical model, and extending the observation time, it will get more high-precision global terrestrial water storage and global ocean bottom pressure to get more detailed information of global mass transport and distribution.

Acknowledgements

The author thanks the GRACE and ECCO team for providing the data. The GRACE data are available at http://grace.jpl.nasa.gov. This work was supported by the National Keystone Basic Research Program (MOST 973) Sub-Project (Grant No. 2012CB72000), National Natural Science Foundation of China (NSFC) (Grant No.11043008), Main Direction Project of Chinese Academy of Sciences (Grant No.KJCX2-EW-T03), and National Natural Science Foundation of China (NSFC) Project (Grant No. 11173050).

Author details

Shuanggen Jin[1*]

Address all correspondence to: sgjin@shao.ac.cn

1 Shanghai Astronomical Observatory, Chinese Academy of Sciences, China

References

[1] Baker, Robert. M. L. (1960). Orbit determination from range and range-rate data. *The Semi-Annual Meeting of the American Rocket Society, Los Angeles.*

[2] Bingham, R. J., & Hughes, C. W. (2006). Observing seasonal bottom pressure variability in the North Pacific with GRACE. *Geophys. Res. Lett.*, 33, L08607, doi: 10.1029/2005GL025489.

[3] Chao, B., Au, A., Boy, J., & Cox, C. (2003). Time-variable gravity signal of an anomalous redistribution of water mass in the extratropic Pacific during 1998-2002. *Geochemistry Geophysics Geosystems*, 4(11), 1096, doi:10.1029/2003GC000589.

[4] Chambers, D. P., Wahr, J., & Nerem, R. S. (2004). Preliminary observations of global ocean mass variations with GRACE, Geophys. *Res. Lett.*, 31, L13310, doi: 10.1029/2004GL020461.

[5] Cheng, M, & Tapley, B. D. (2004). Variations in the Earth's oblateness during the past 28 years. *J. Geophys. Res.*, 109, B09402, doi:10.1029/2004JB003028.

[6] Chlieh, M., Avouac, J. P., Hjorleifsdottir, V., et al. (2007). Coseismic slip and afterslip of the great (Mw 9.15) Sumatra-Andaman earthquake of 2004. *Bull. Seismol. Soc. Am.*, 97(1A), S 152-S173.

[7] Dickey, J. O., Bentley, C. R., Bilham, R., et al. (1999). Gravity and the hydrosphere: new frontier. *Hydrological Sciences Journal*, 44(3), 407-415.

[8] ESA, Reports for Mission Selection. (1999). Gravity Field and Steady-State Ocean Circulation Mission. SP-1233(1), *ESA Publication Division, ESTEC*, Noordwijk, The Netherlands (available from web site, http://www.esa.int/livingplanet/goce.

[9] Flechtner, F. (2007). AOD1B Product Description Document for Product Releases 01 to 04, GRACE 327-750. *CSR publ. GR-GFZ-AOD-0001 Rev. 3.1, University of Texas at Austin*, 43.

[10] Frappart, F., Calmanta, S., Cauhopéa, M., et al. (2006). Preliminary results of ENVISAT RA-2- derived water levels validation over the Amazon basin. *Remote Sensing of Environment*, 100, 252-264.

[11] Fukumori, I., Lee, T., Menemenlis, D., et al. (2000). A dual assimilation system for satellite altimetry. *paper presented at Joint TOPEX/Poseidon and Jason-1 Science Working Team Meeting, NASA, Miami Beach, Fla.*, 15-17, Nov.

[12] Gill, A., & Niiler, P. (1973). The theory of seasonal variability in the ocean. *Deep-Sea Research*, 20, 141-177.

[13] Han, D., & Wahr, J. (1995). The viscoelastic relaxation of a realistically stratified earth, and a further analysis of post-glacial rebound. *Geophysical J. Int.*, 120, 287-311.

[14] Han, S. C., Shum, C. K., Bevis, M., et al. (2006). Crustal dilatation observed by GRACE after the 2004 Sumatra-Andaman earthquake. *Science*, 313(5787), 658-666, doi:10.1126/science.1128661.

[15] Heiskanen, W. A., & Moritz, H. (1967). Physical Geodesy. *Freeman, San Francisco.*

[16] Hopkin, M. (2005). Triple slip of tectonic plates caused seafloor surge,. *Nature*, 433(3), doi:10.1038/433003b.

[17] Jin, S.G., Chambers, D.P., & Tapley, B.D. (2010). Hydrological and oceanic effects on polar motion from GRACE and models. *J.Geophys. Res.*, 115, B02403, doi: 10.1029/2009JB006635.

[18] Jin, S.G., Zhang, L, & Tapley, B. (2011). The understanding of length-of-day variations from satellite gravity and laser ranging measurements. *Geophys. J. Int.*, 184(2), 651-660, doi:10.1111/j.1365-246X.2010.04869.x, 1365-246.

[19] Leuliette, E, Nerem, R, & Russell, G. (2002). Detecting time variations in gravity associated with climate change. *J. Geophys. Res.*, 107, B62112, doi:10.1029/2001JB000404.

[20] Losch, M., Adcroft, A. J., & Campin, M. (2004). How sensitive are coarse general circulation models to fundamental approximations in the equations of motion? *J. Phys. Oceanogr.*, 34, 306-319.

[21] Luthcke, S. B., Zwally, H. J., Abdalati, W., et al. (2006). Recent Greenland ice mass loss by drainage system from satellite gravity observations,. *Science*, 314, 1286-1289.

[22] Marshall, J., Adcroft, A., Hill, C., et al. (1997). A finite-volume, incompressible, Navier Stokes model for studies of the ocean on parallel computers. *J. Geophys. Res.*, 102, 5753-5766.

[23] Paulson, A, Zhong, S, & Wahr, J. (2007). Inference of mantle viscosity from GRACE and relative sea level data. *Geophys. J. Int.*, doi:10.1111/j.1365-246X.2007.03556.x, 171, 497-508.

[24] Park, J. H., Watts, D. R., Donohue, K. A., et al. (2008). A comparison of in situ bottom pressure array measurements with GRACE estimates in the Kuroshio Extension. *Geophys. Res. Lett.*, 35, L17601, doi:10.1029/2008GL034778.

[25] Pollitz, F. F. (2006). A new class of earthquake observations. *Science*, 313(619), doi: 10.1126/science.1131208.

[26] Ponte, R. M., Quinn, K. J., Wunsch, C., et al. (2007). A comparison of model and GRACE estimates of the large-scale seasonal cycle in ocean bottom pressure. *Geophys. Res. Lett.*, doi:10.1029/2007GL029599, 34, L09603.

[27] Ramillien, G., Cazenave, A., & Brunau, O. (2004). Global time variations of hydrological signals from GRACE satellite gravimetry. *Geophys. J. Int.*, 158(3), 813-826.

[28] Ray, R. D., & Luthcke, S. B. (2006). Tide model errors and GRACE gravimetry: Towards a more realistic assessment. *Geophys. J. Int.*, 167, 1055-1059.

[29] Reigber, Ch., Schwintzer, P., & Luhr, H. (1999). The CHAMP geopotential mission. *Boll. Geof. Teor. Appl.*, 40, 285-289.

[30] Rietbroek, R., Le Grand, P., Wouters, B., et al. (2006). Comparison of in situ bottom pressure data with GRACE gravimetry in the Crozet-Kerguelen region. *Geophys Res Lett.*, 33, L21601.

[31] Rodell, M., Houser, P. R., Jambor, U., et al. (2004). The Global Land Data Assimilation System. *Bull. Amer. Meteor. Soc.*, 85(3), 381-394, doi: BAMS-85-3-381.

[32] Rodell, M., Velicogna, I., & Famiglietti, J. S. (2009). Satellite-based estimates of groundwater depletion in India. *Nature*, 460, 999-1002, doi: 10.1038/nature08238.

[33] Simons, M., & Hager, B. H. (1997). Localization of the gravity field and the signature of glacial rebound. *Nature*, 390(6659), 500-504.

[34] Swenson, S, Chambers, D, & Wahr, J. (2008). Estimating geocenter variations from a combination of GRACE and ocean model output. *J. Geophys. Res.*, 113, B08410, doi: 10.1029/2007JB005338.

[35] Swenson, S, & Wahr, J. (2002). Methods for inferring regional surface-mass anomalies from Gravity Recovery and Climate Experiment (GRACE) measurements of time-variable gravity. *J. Geophys. Res.*, 107, B92193, doi:10.1029/2001JB000576.

[36] Swenson, S C., & Wahr, J. (2006). Post-processing removal of correlated errors in GRACE data. *Geophys. Res. Lett.*, 33(L08402), doi:10.1029/2005GL025285.

[37] Tapley, B. D., Bettadpur, S., Ries, J. C., et al. (2004). GRACE measurements of mass variability in the Earth system. *Science*, 305(568), 503-505.

[38] Tapley, B. D., & Reigber, Ch. (2001). The GRACE Mission: Status and future plans. *Eos Trans, AGU*, 82(47), Fall Meet. Suppl., G41 C-02.

[39] Velicogna, I., & Wahr, J. (2006). Measurements of time-variable gravity show mass loss in Antarctica,. *Science*, 311, 1745-1756, doi:10.1126/science.1123785.

[40] Wahr, J., Molenaar, M., & Bryan, F. (1998). Time-variability of the Earth's gravity field: Hydrological and oceanic effects and their possible detection using GRACE. *J. Geophys. Res.*, 103(32), 205-30.

[41] Washington, W. M., Weatherly, J. W., Meehl, G. A., et al. (2000). Parallel climate model (PCM) control and transient simulations. *Climate Dynamics*, 16, 755-774.

[42] Watkins, M., & Bettadpur, S. (2000). The GRACE mission: challenges of using micron-level satellite-to-satellite ranging to measure the Earth's gravity field. *Proc. of the International Symposium on Space, Dynamics, Biarritz, France, Center National d'Etudes Spatiales (CNES), Delegation a la Communication (pub1.)*.

[43] Wolff, M. (1969). Direct Measurement of the Earth's Gravitational Potential Using a Satellie Pair. *J. Geophys. Res.*, 74(22), 5295-5300, doi:10.1029/JB074i022p05295.

[44] Yoder, C. F., Williams, J. G., Dickey, J. O., et al. (1983). Secular variation of Earth's gravitational harmonic J coefficient from Lageos and non-tidal acceleration of Earth rotation. *Nature*, 303, 757-762.